SAND2014-17863J

Electronic structure modeling of InAs/GaSb superlattices with hybrid density functional theory

T. Garwood,[1, a)] N. A. Modine,[2, b)] and S. Krishna[1, c)]
[1)] *Center for High Technology Materials, University of New Mexico, Albuquerque, New Mexico 87106-4343, USA*
[2)] *Sandia National Laboratories, Albuquerque, New Mexico 87185-1315, USA*

(Dated: 12 September 2014)

We present bandgap data for various InAs/GaSb type-II superlattice structures calculated using the generalized Kohn-Sham formulation of density functional theory. A PBE0-type hybrid functional was used, and the portion of the exact exchange was tuned to fit the bandgaps of the binary compounds InAs and GaSb with the best agreement to bulk experimental values obtained with 18% of the exact exchange. The heterostructures considered in this study are 6 monolayer (ML) InAs / 6ML GaSb, 8ML InAs / 8ML GaSb and 10ML InAs / 10ML GaSb with deviations from the experimental bandgaps ranging from 3% to 11%.

InAs/GaSb type-II strained layer superlattices (SLS) have attracted considerable research interest for use as mid-and long-wavelength infrared photodetectors.[1] The absorption wavelength of these superlattices can be tuned between 3μm and 32μm, depending on the thicknesses of the constituent InAs and GaSb layers.[2–4] InAs/GaSb SLS also exhibit comparable quantum efficiency and lower Auger current than bulk HgCdTe detectors of comparable bandgap.[5–7] Superior performance of InAs/GaSb SLS photodetectors has been expected based on theoretical arguments, but is yet to be observed experimentally. The reason this theoretical potential has not been achieved is that current InAs/GaSb SLS devices display a high level of dark current, which is associated with shorter carrier lifetimes. The high rate of carrier recombination in InAs/GaSb devices is generally attributed to unidentified defects present in the devices.[8]

The exact mechanism for the defect induced recombination is currently unknown, however, it is expected to involve transitions to a defect energy level near the middle of the small bandgap of the SLS structures. Experiments suggest that the performance limiting defects are associated with gallium as gallium-free (InAs/InAsSb) SLS structures exhibit longer carrier lifetimes.[9,10] High-Resolution Transmission Electron Microscopy images of InAs/GaSb SLS structures depict what appear to be isolated In and As atoms in the GaSb layers and, conversely, Ga and Sb atoms in the InAs layers.[11] Accurate defect level calculations are needed to determine whether isoelectric substitutions account for the recombination mechanism or whether some other type of defect (e.g., anti-sites or interstitials) are responsible.

First-principles calculations of point defects and impurities in semiconductors, insulators, and metals have become an integral part of materials research over the last few decades.[12–14] One of the more popular methods of calculating defect levels uses Kohn-Sham Density Functional Theory (DFT).[15] Calculations are typically performed in a supercell that contains a defect surrounded by bulk material, and periodic boundary conditions are applied at the supercell boundaries. The results are then processed to remove interactions between the periodically repeated cells.[16–20] Charges are added or removed from the computational cell in order to create defect charge states, and the energy differences between different charge states can be used to calculate the defect levels, which are the values of the Fermi level at which the defect charge state changes. The presence and position of defect levels within the band gap of the host material has a dramatic effect on the rate of carrier recombination induced by the defect. When applied with reasonable care, this approach has a good record of predicting defect levels that agree with experimental measurements to within a few tenths of an electron volt.[21–26]

Despite this record of success for defects in a variety of semiconductors, conventional DFT functionals, based on the local density and generalized gradient approximations (LDA and GGA), give vanishing band gaps for InAs, GaSb[28], and, as we report in this work, InAs/GaSb superlattices and thus cannot be expected to give accurate results for defect levels in these materials. Although the use of finite supercells can effectively increase the range of defect levels that can be obtained with DFT beyond the Kohn-Sham band gap[27], charge will almost certainly be lost from the defect to the delocalized band edge states when the Kohn-Sham gap is zero. In contrast, hybrid functionals, e.g., PBE0, B3LYP, and HSE06, have been shown to give more accurate band gaps for bulk semiconductors, including narrow band gap semiconductors such as InAs and GaSb.[29–31] Accurate calculations for the band gaps of InAs/GaSb SLS, where the superlattice minibands are only separated by a few tenths of an eV, can be expected to be even more challenging. In addition to bulk band gaps, accurate calculations of SLS band gaps require an accurate treatment of a number of other properties of the constituent materials such as band masses and band offsets. The $\mathbf{k}\cdot\mathbf{p}$ theory has been successfully used to calculate accurate band gaps for InAs/GaSb SLS.[32–35] However, the $\mathbf{k}\cdot\mathbf{p}$ theory is

[a)] Electronic mail: tgarwood@unm.edu
[b)] Electronic mail: namodin@sandia.gov
[c)] Electronic mail: skrishna@chtm.unm.edu

a continuum theory that lacks a representation for specific atoms, and therefore, there is no straightforward approach to predict the properties of point defects for which the local atomistic structure differs significantly from the host crystal. Thus, an accurate first principles approach to calculating the properties of SLS structures would be invaluable.

In this letter, we investigate the accuracy of InAs/GaSb superlattice bandgap calculations using hybrid DFT functionals. We will first report the technical parameters used in the bulk and superlattice DFT calculations performed for this study. We then will discuss our band-gap and lattice constant results for bulk InAs and GaSb and our procedure for optimizing the mixing factor used in our PBE0-like functional. Next, we will describe our procedure for performing hybrid superlattice calculations, which will be followed by our calculated results for the band gaps of three InAs/GaSb SLS and discussion of these results.

FIG. 1. Ball-and-stick model of the type of structure used in our DFT calculations for InAs / GaSb SLS made using VESTA software.[36] The SLS shown below is a 4 ML InAs / 4 ML GaSb SLS where the top half is InAs and the bottom half is GaSb. In order from dark to light, the balls represent the atoms: In, Ga, As, Sb.

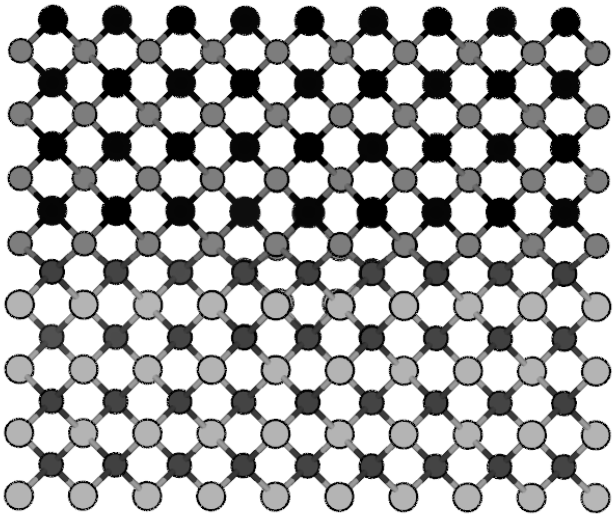

Our hybrid DFT calculations were performed using the open-source Socorro DFT package.[37] A plane wave basis with a 40 Rydberg cutoff was used to represent the valence Kohn Sham orbitals, and norm conserving pseudopotentials (NCPs) were used to represent the effect of the nuclei and atomic cores on the valence electrons. The NCPs were constructed for the PBE exchange-correlation functional using the fhi98PP[38,39] code with three electrons treated as valence (ns^2 and np^1) for Ga ($n = 4$) and In ($n = 5$), and five electrons treated as valence (ns^2 and np^3) for As ($n = 4$) and Sb ($n = 5$). The In pseudopotential used in our calculations was obtained from the Abinit website.[40] Monkhorst-Pack[41] k-point meshes shifted to include the Γ point were used to sample the Brillouin zone with a 8x8x8 mesh used for bulk unit cells and a 4x4x1 mesh used for the SLS structures. Occupations of the Kohn Sham orbitals were calculated using a Fermi distribution with $T = 79K$. The atomic positions of the superlattice structures were relaxed until the total energies no longer changed at the 1 meV level. The integrable singularity occurring in the Fock exchange for periodic systems was calculated using the method of Spencer and Alavi.[42]

TABLE I. Calculated DFT results vs. experimental lattice constant (L_0) and Band Gap (E_0).[43]

Material	PBE	PBE18%	Exp.
InAs L_0 (Å)	6.18	6.17	6.06
GaSb L_0 (Å)	6.21	6.15	6.10
InAs E_0 (eV)	——	0.39	0.35
GaSb E_0 (eV)	——	0.69	0.73

Table I compares the lattice constants and bandgaps for InAs and GaSb calculated using the PBE functional and an optimized hybrid functional (to be described below) with experimental results. PBE predicts InAs and GaSb to be metallic due to the collapse of the band gap in a small region near the Γ point of the Brillouin zone, and thus we did not include these results in Table I. The hybrid functional used in this study was a modified version of PBE0.[44,45] This functional is constructed by the mixing of a fraction α of the Fock exchange with a fraction $1 - \alpha$ of the PBE exchange. The exchange-correlation energy E_{xc} can then be expressed in this simple form:

$$E_{xc} = \alpha E_x + (1 - \alpha)E_x^{PBE} + E_c^{PBE} \quad (1)$$

where E_x is the Fock exchange, E_x^{PBE} is the PBE exchange, and E_c^{PBE} is the PBE correlation. In standard PBE0, the mixing coefficient α is taken to be 25%. However, the band gaps of narrow band gaps semiconductors such as InAs and GaSb are significantly too large when this value is used.[46] Due to the difficulty in accurately determining the very small separations between minibands, we optimized the PBE hybrid mixing factor to fit the bandgaps of InAs and GaSb and found that the mixing factor $\alpha = 0.18$ splits the error in the band gap between InAs and GaSb with InAs being 0.04 eV too large and GaSb being 0.04 eV too small (see Table I).

The InAs / GaSb superlattices were represented in our DFT calculations by atomistic structures similar to the ball-and-stick model of a 4 ML InAs / 4 ML GaSb SLS shown in Fig.1. The fundamental unit cell of the SLS in Fig. 1 is periodically repeated to show the bonding pattern. The number of layers of each material was adjusted to give 6 ML InAs / 6 ML GaSb, 8 ML InAs / 8 ML GaSb, and 10 ML InAs / 10 ML GaAs SLS structures in our calculations. For efficiency, we included one atom in each layer of the SLS in our DFT calculations, and

Brillouin zone sampling was used to capture the effects of the periodically repeated structure. Due to the computational expense of the hybrid functional, we optimized the atomic positions and growth-direction lattice constant, L_z, of the superlattices using the semi-local PBE functional. The lattice constants perpendicular to the growth direction L_x and L_y were fixed at the lattice constant of the substrate. For this purpose, the PBE lattice constant of InAs obtained from our bulk calculations was used. This is consistent with our relaxation of the atomic positions using the PBE functional. The PBE total energy of the relaxed superlattice was obtained for a range of L_z values, and least-squares fitting to a quadratic function was used to find the L_z value that minimized the energy. L_z was then fixed at this value, and the atomic positions were relaxed using PBE once more. We then used our optimized hybrid functional to calculate the band gaps of the SLS structures with the lattice constants and atomic positions fixed at these values.

TABLE II. Band gap results obtained for 6 monolayer (ML) InAs /6 ML GaSb, 8 ML InAs / 8 ML GaSb and 10 ML InAs / 10 ML GaSb using PBE0 with a 18% mixing factor. Calculated results are compared to experimental values for 6 ML InAs / 6 ML GaSb[47], 8 ML InAs / 8 ML GaSb[48] and 10 MLInAs/10 MLGaSb.[49]

Material	Calc. E_0 (eV)	Exp. E_0 (eV)	Error	% Error
6InAs/6GaSb	0.37	0.36	0.01	2.8
8InAs/8GaSb	0.30	0.27	0.03	11.1
10InAs/10GaSb	0.25	0.23	0.02	8.7

FIG. 2. Band gap results obtained for 6 ML InAs / 6 ML GaSb, 8 ML InAs / 8 ML GaSb and 10 ML InAs / 10 ML GaSb using PBE0 with a 18% mixing factor. Calculated results are compared to experimental values for 6 ML InAs / 6 ML GaSb[47], 8 ML InAs / 8 ML GaSb[48] and 10 ML InAs / 10 ML GaSb.[49]

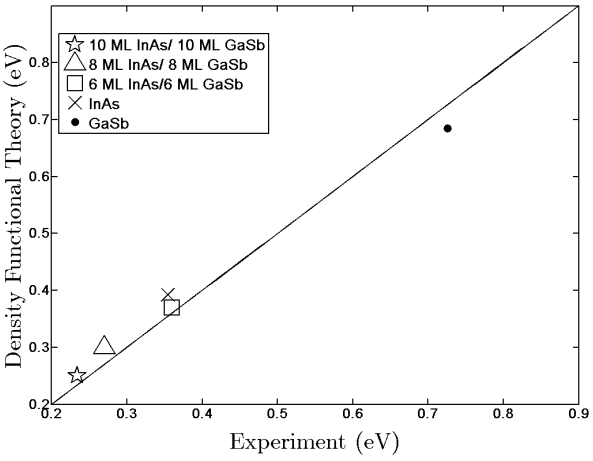

The bandgaps obtained using this procedure, as well as experimental values, are reported in Table II and Fig. 2. Our calculated bandgaps for InAs/GaSb superlattices are within 30 meV of values obtained from experiment. Due to the small band gaps of InAs/GaSb SLS, these absolute errors correspond to relative errors of 4-9% . These errors are smaller than those commonly obtained for bulk III-V compounds using the best off-the-shelf hybrid functionals, which shows the value of our optimization of the functional in calculations for these ultra narrow band gap systems.

Our study shows that DFT can be used to predict bandgap in quantum well heterostructures with good precision. This indicates that defect charge states will not be corrupted by an unphysical loss of charge to the extended, band edge states. As mentioned above, this result also requires that the hybrid calculations are getting a number of properties of InAs and GaSb correct in addition to the band gaps. This suggests that defects will interact with the superlattice structure in a realistic fashion and that the behavior of defect in these structures will be accurately reproduced.

This work was performed, in part, at the Center for Integrated Nanotechnologies, an Office of Science User Facility operated for the U.S. Department of Energy (DOE) Office of Science. Sandia National Laboratories is a multi-program laboratory managed and operated by Sandia Corporation, a wholly owned subsidiary of Lockheed Martin Corporation, for the U.S. Department of Energy's National Nuclear Security Administration under contract DE-AC04-94AL85000.

[1] E. Plis, J. B. Rodriguez, and S. Krishna, Type-II superlattice detectors. *Comprehensive Semiconductor Science and Technology* 6:229, (2011)

[2] C. Cervera, I. Ribet-Mohamed, R. Taalat, J. P. Perez, P. Christol, and J. B. Rodriguez, Dark current and noise measurements of an InAs/GaSb superlattice photodiode operating in the midwave infrared domain, Journal of Electronic Materials, vol. 41, pp. 27142718, 2012.

[3] N. Gautam, H. S. Kim, M. N. Kutty, E. Plis, L. R. Dawson, and S. Krishna, Performance improvement of longwave infrared photodetector based on type-II InAs/GaSb superlattices using unipolar current blocking layers, Applied Physics Letters, vol. 96, no. 23, Article ID 231107, 2010.

[4] Y. Wei, A. Gin, M. Razeghi, and G. J. Brown, Advanced InAs/GaSb superlattice photovoltaic detectors for very long wavelength infrared applications, Applied Physics Letters, vol. 80, no. 18, pp. 32623264, 2002.

[5] B.-M. Nguyen, D. Hoffman, Y. Wei, P.-Y. Delaunay, A. Hood, and M. Razeghi, Very high quantum efficiency in type-II InAs/GaSb super- lattice photodiode with cutoff of 12μm, Appl. Phys. Lett., vol. 90, no. 23, p. 231108, 2007.

[6] Y. Wei, A. Hood, H. Yau, A. Gin, M. Razeghi, M. Z. Tidrow, and V.Nathan, Uncooled operation of type-II InAs/GaSb superlattice photodiodes in the midwavelength infrared range, Appl. Phys. Lett. , vol. 86, no. 23, p. 233106, 2005.

[7] A. Khoshakhlagh, J.B. Rodriguez, E. Plis, G.D. Bishop, Y.D. Sharma, H. S. Kim, L. R. Dawson, and S. Krishna, Bias dependent dual band response from InAs/Ga(In)Sb type II strain layer superlattice detectors, Appl. Phys. Lett. , vol. 91, no. 26, p. 263504, 2007.

[8] Donetsky, Dmitry, Stefan P. Svensson, Leonid E. Vorobjev, and Gregory Belenky. "Carrier lifetime measurements in short-period InAs/GaSb strained-layer superlattice structures." Applied Physics Letters 95, no. 21 (2009): 212104.

[9]E. H. Steenbergen, Y. Huang, J.-H. Ryou, L. Ouyang, J.-J. Li, D. J. Smith, R. D. Dupuis, and Y.-H. Zhang, Structural and optical characterization of type-II InAs/$InAs_{1-x}Sb_x$ superlattices grown by metalorganic chemical vapor deposition.
[10]Aytac, Y., B. V. Olson, J. K. Kim, E. A. Shaner, S. D. Hawkins, J. F. Klem, M. E. Flatt, and T. F. Boggess. "Effects of layer thickness and alloy composition on carrier lifetimes in mid-wave infrared InAs/InAsSb superlattices." Applied Physics Letters 105, no. 2 (2014): 022107.
[11]E. Luna, B. Satpati, J. B. Rodriguez, A. N. Baranov, E. Tourni, and A. Trampert, Applied Physics Letters **96**, 021904 (2010)
[12]Van de Walle, C.G. and Neugebauer, J. (2004) J. Appl. Phys., 95, 3851.
[13]Drabold, D.A. and Estreicher, S.K. (eds) (2007) Theory of Defects in Semiconductors, Springer-Verlag, Berlin.
[14]Asato, M., Mizuno, T., Hoshino, T., Masuda-Jindo, K., and Kawakami, K. (2001) Mater. Sci. Eng. A, 312, 72.
[15]W. Kohn, L.J. Sham, Phys. Rev. 140 (1965) A1133
[16]C. Freysoldt, J. Neugebauer, and C.G. Van de Walle, Phys. Status Solidi B **248**, 1067 (2011).
[17]H.P. Komsa, T.T. Rantala, and A. Pasquarello, Phys. Rev. B **86**, 045112 (2012).
[18]S. Lany and A. Zunger, Phys. Rev. B **78**, 235104 (2008).
[19]A. F. Wright and N. A. Modine, Phys. Rev. B **74**, 235209 (2006).
[20]J. Lento, J.L. Mozos, and R. M. Nieminen, J. Phys.: Condens. Matter **14**, 2637 (2002).
[21]Payne, M., Teter, M.P., Allan, D.C., Arias, T.A., and Joannopoulos, J.D. (1992) Rev. Mod. Phys., 64, 1045.
[22]A. Alkauskas, P. Broqvist, and A. Pasquarello, Phys. Rev. Lett. **101**, 046405 (2008).
[23]P.A. Schultz, Phys. Rev. Lett. **96**, 246401 (2006).
[24]P.A. Schultz and O.A. von Lilienfeld, Modelling Simul. Mater. Sci. Eng. **17**, 084007 (2009).
[25]A. F. Wright, Phys. Rev. B **74**, 165116 (2006).
[26]R.R. Wixom and A.F. Wright, Phys. Rev. B **74**, 205208 (2006).
[27]N. A. Modine, A. F. Wright, and S. R. Lee, Comput. Mater. Sci. **92**, 431 (2014).
[28]J.P. Perdew, M. Levy. Phys. Rev. Lett., 51 (1983), p. 1884
[29]J. Heyd, J. E. Peralta, G. E. Scuseria, and R. L. Martin. Energy band gaps and lattice parameters evaluated with the Heyd-Scuseria-Ernzerhof screened hybrid functional *J. Chem. Phys.* **123**, 174101 (2005);
[30]S. Tomi and N. M. Harrison. Electronic structure of IIIVs semiconductors from B3LYP and PBE0 functionals *AIP Conf. Proc.* **1199**, 65 (2010);
[31]G. Kresse, F. Tran, Y.-S. Kim, M. Marsman, and P. Blaha. Towards efficient band structure and effective mass calculations for III-V direct band-gap semiconductors. *Phys. Rev. B*, 82:205212, (2010)
[32]M.-E. Pistol and C. Pryor, Band-edge diagram for strained III-IV semiconductor quantum wells, wires, and dots, *Phys. Rev. B* **72**, 205311 (2005).
[33]P.C. Klipstein, Y. Livneh, O. Klin, S. Grossman, N. Snapi, A. Glozman, E. Weiss. A k•p model of InAs/GaSb type II superlattice infrared detectors. *Infrared Phys. & Tech.* **59** (2013), p. 53-59
[34]Wang, L.-W. and Wei, S.-H. and Mattila, T. and Zunger, A. and Vurgaftman, I. and Meyer, J. R. Multiband coupling and electronic structure of $(InAs)_n/(GaSb)_n$ superlattices. *Phys. Rev. B* **60**, (1999)
[35]H. S. Kim, Ph.D. thesis, University of New Mexico, Albuquerque, 2010.
[36]K. Momma and F. Izumi, "VESTA 3 for three-dimensional visualization of crystal, volumetric and morphology data," J. Appl. Crystallogr., 44, 1272-1276 (2011).
[37]See <http://dft.sandia.gov/socorro>.
[38]See <http://www.fhi-berlin.mpg.de/th/fhi98PP/>.
[39]M. Fuchs, M. Scheffler, Comput. Phys. Commun. 119, 67 (1999) "Ab initio pseudopotentials for electronic structure calculations of poly-atomic systems using density-functional theory".
[40]See <http://www.abinit.org/downloads/psp-links/psp-links/gga_fhi>.
[41]H. J. Monkhorst and J. D. Pack, *Phys. Rev. B* **13**, 5188 (1976).
[42]J. Spencer and A. Alavi, Phys. Rev. B **77**, 193110 (2008).
[43]See <http://www.ioffe.ru/SVA/NSM/Semicond/>.
[44]C. Adamo and V. Barone. Toward reliable density functional methods without adjustable parameters: The PBE0 model J. Chem. Phys. 110, 6158 (1999)
[45]J. P. Perdew, M. Ernzerhof, and K. Burke. J. Chem. Phys. http://dx.doi.org/10.1063/1.472933 105, 9982 (1996). Rationale for mixing exact exchange with density functional approximations.
[46]S. Tomic and N. M. Harrison, AIP Conference Proceedings **1199**, 65 (2010). *App. Phys. Lett.*, 99(7):071111, (2011)
[47]B. Klein, N. Gautam, S. Myers, S. Krishna, "Temperature-dependent absorption derivative on InAs/GaSb Type II superlattices", in Infrared Technology and Applications XXXVIII, Bjrn F. Andresen; Gabor F. Fulop; Paul R. Norton, Editors, Proceedings of SPIE Vol. 8353 (SPIE, Bellingham, WA 2012), 83530X.
[48]R. Kaspi, C. Moeller, A. Ongstad, M. L. Tilton, D. Gianardi, G. Dente, and P. Gopaladasu, Applied Physics Letters 76, 409 (2000); doi: 10.1063/1.125770
[49]B. Klein, E. Plis, M. N. Kutty, N. Gautam, A. Albrecht, S. Myers and S. Krishna, Phys. D: Appl. Phys. **44** (2011) 075102 (5pp)